

# Analytical Methods

Accepted Manuscript



This is an *Accepted Manuscript*, which has been through the Royal Society of Chemistry peer review process and has been accepted for publication.

*Accepted Manuscripts* are published online shortly after acceptance, before technical editing, formatting and proof reading. Using this free service, authors can make their results available to the community, in citable form, before we publish the edited article. We will replace this *Accepted Manuscript* with the edited and formatted *Advance Article* as soon as it is available.

You can find more information about *Accepted Manuscripts* in the [Information for Authors](#).

Please note that technical editing may introduce minor changes to the text and/or graphics, which may alter content. The journal's standard [Terms & Conditions](#) and the [Ethical guidelines](#) still apply. In no event shall the Royal Society of Chemistry be held responsible for any errors or omissions in this *Accepted Manuscript* or any consequences arising from the use of any information it contains.

1  
2  
3  
4 1 **Highly Sensitive Fluorescent Aptasensor for *Salmonella paratyphi A***  
5  
6 2 **Via DNase I-mediated Cyclic Signal Amplification**  
7  
8  
9 3

10  
11 4 Xing Yan<sup>a</sup>, Wenkai Li<sup>a,b</sup>, Keyi Liu<sup>a</sup> and Le Deng<sup>a,1</sup>  
12  
13  
14 5

15  
16 <sup>a</sup> Department of Microbiology, College of Life Science, Hunan Normal University, Changsha,  
17  
18 Hunan, 410081, China.  
19

20  
21 <sup>b</sup> Department of Biochemistry, The State Key Laboratory of Medical Genetics & School of  
22  
23 Life Science, Central South University, Changsha, Hunan, 410013, China.  
24  
25

26 10  
27  
28

29 11  
30  
31

32 12  
33  
34

35 13  
36  
37

38 14  
39  
40

41 15  
42  
43

44 16  
45  
46

47 17  
48  
49

50 18  
51  
52

53 19  
54  
55

---

56 <sup>1</sup> Corresponding author. Department of Microbiology, College of Life Science, Hunan Normal University, Changsha, Hunan,  
57 410081, China. Tel: 86 731 88872927; Fax: 86 731 88883310; E-mail address: dengle@hunnu.edu.cn.  
58 E-mail address for each author: Xing Yan: 1071907250@qq.com; Wenkai Li: wenkaili@163.com; Keyi Liu:  
59 kevenlky@qq.com.  
60

**Abstract**

Outbreaks of *Salmonella paratyphi A* (*S. paratyphi A*) infection continue to occur worldwide and have drawn close attention. A useful practical detection platform is essential to the early rapid diagnosis of the infection. In this study, a simple and cost-effective DNA aptasensor was constructed, which was composed of a designed aptamer (DA) and two short carboxyfluorescein(FAM)-modified sequences (probe 1 and probe 2) for fluorimetric determination of *S. paratyphi A*. In the absence of target, the two-FAMs aptasensor (the aptasensor) was bound to graphene oxide (GO) and the fluorescence of FAM was quenched. In the presence of target, however, the aptasensor was released from the surface of GO due to specific binding of the aptasensor to the target and a strong fluorescent signal could be detected subsequently. More importantly, the fluorescent signal could be substantially amplified by a DNase I-mediated target recycling process. Under the optimized conditions, the fluorescence intensity increased linearly with the target concentrations ranging from  $1 \times 10^2$  to  $1 \times 10^{11}$  cells/mL with a detection limit of  $1 \times 10^2$  cells/mL. These results demonstrated that this detection platform exhibited high sensitivity and specificity in the detection of *S. paratyphi A*, and it might even be a potential alternative approach for other bacteria detection.

**Keywords**

Aptasensor, Fluorescence intensity, *Salmonella paratyphi A*, Graphene oxide, DNase I, Target recycling.

## 1. Introduction

Salmonella is one of the zoonotic pathogenic bacteria in the field of public hygienics<sup>[1]</sup>. It often causes different degrees of poultry and animal infections as well as human diseases by food-borne contamination. As a timely treatment of Salmonella infection is difficult, it is required to develop a rapid detection for them<sup>[2]</sup>. As a food-borne pathogen which could be transmitted by domestic water, food, fly, cockroach and so forth<sup>[3]</sup>, *S. paratyphi A* brings about a large variety of health problems, from minor manifestations such as headache, fever, anepithymia, to more serious complications of enterorrhagid, enterobrosis, myocarditis that lead to high death rate in humans. Since Salmonella was initially identified as human pathogenic bacterium in the late 19th century, testing methodologies were all based on the tests that used feces or blood from infected patients as clinical specimens<sup>[4]</sup>. However, these conventional standard detection methods have their limitations. For instance, routine inspection and bacteriological examination are time-consuming and labor intensive, generally with a week. Immunological methods are costly, require complex procedures and produce false-positive results from cross-reaction, increasing the challenge in practical application<sup>[5]</sup>. Molecular biological methods have also some disadvantages. Polymerase Chain Reaction (PCR), for instance, requires multiple touch conditions and produces some contaminations during nucleic acid sample extraction<sup>[6]</sup>. Although Amplified Fragment Length Polymorphism (AFLP) is also applied to microorganism researches<sup>[7]</sup>, there are limited reports about detection of Salmonella. Therefore, it is necessary to develop a time-saving method with high sensitivity and specificity for *S. paratyphi A* detection.

Aptamers are single-stranded DNA (ssDNA) or RNA molecules obtained from nucleic acid

1  
2  
3  
4 64 pool by the Systematic Evolution of Ligands by Exponential Enrichment (SELEX) procedure  
5  
6 65 in vitro, which can bind to various kinds of targets, including ions, proteins, whole cells and  
7  
8 66 small molecules, with high specificity, sensitivity and affinity<sup>[8]</sup>. They have been used as  
9  
10 67 biomarkers and therapeutic agents, and provide alternative element for ligand recognition in  
11  
12 68 diagnosis and detection systems as compared to antibodies<sup>[9]</sup>. Meanwhile, all kinds of targets  
13  
14 69 have been detected based on aptamer recently, including bacteria, adenosine triphosphate  
15  
16 70 (ATP), proteins, cells, ions, molecules<sup>[10-15]</sup>, etc. In short, aptamers have extensive application  
17  
18 71 prospects in detection and therapy fields<sup>[16,17]</sup>.

19  
20  
21  
22  
23  
24 72 Many enzymes have been used for determination, including DNA polymerase,  
25  
26 73 exonuclease and endonuclease. DNase I is an endonuclease that can digests single- and  
27  
28 74 double-stranded sequences of DNA (ssDNA and dsDNA) simultaneously and randomly. It  
29  
30 75 hydrolyzes phosphodiester bonds, producing mono- and oligodeoxyribonucleotides with  
31  
32 76 5'-phosphate and 3'-OH groups. In the presence of  $Mg^{2+}$ , it cleaves each strand of dsDNA  
33  
34 77 independently in a statistically random fashion. Compared to other endonucleases, it requires  
35  
36 78 no specific recognition site and possesses a broad hydrolytic spectrum. Although it has some  
37  
38 79 applications in many detection systems, its few works are reported in bacterial detection<sup>[18]</sup>.

39  
40  
41  
42  
43  
44 80 Nanomaterials are widely used for detection systems<sup>[19]</sup>. Graphene has attracted great  
45  
46 81 attention for its remarkable properties (electronic, mechanical, and thermal)<sup>[20]</sup>. Graphite is a  
47  
48 82 substance with stratified structure formed by  $SP^2$  carbon hybridization, while graphene is just  
49  
50 83 one layer of graphite. After being treated by concentrated acid or strong oxidant, graphene is  
51  
52 84 oxidized to form GO with hydroxy, carbonyl and epoxy groups. As a monatomic two-  
53  
54 85 dimensional structure, GO has its unique features compared to other quenching nanomaterials:  
55  
56  
57  
58  
59  
60

1  
2  
3  
4 86 Firstly, it can combine with ssDNA by  $\pi$ - $\pi$  stacking non-covalent interactions<sup>[21]</sup>. Secondly, it  
5  
6 87 is able to quench fluorescence with high efficiency and its water-solubility is better. Thirdly,  
7  
8 88 it prevents ssDNAs who adsorb onto the surface of GO from being digested by enzyme in the  
9  
10 89 biologic environment. Hence, GO, as a superb nanomaterial, would be easily used in  
11  
12 90 biosensors for pathogen detection.

13  
14  
15  
16 91 Fluorescence, as a highly sensitive photosignal, has been widely exploited to detect many  
17  
18 92 kinds of materials<sup>[22]</sup>, including tissues, drugs, cells, etc. The fluorescence of FAM could be  
19  
20 93 annihilated by carbon nanomaterials, enabling it is extensively used in detecting *S. paratyphi*  
21  
22 94 *A*<sup>[23,24]</sup>. Generally speaking, fluorescence intensity detected by use of one FAM is limited.  
23  
24  
25  
26 95 However, when two FAMs are simultaneously used, the fluorescence would enhanced  
27  
28 96 considerably due to superimposed effect of the fluorescence. Supposing that we employed  
29  
30 97 enzymes to recycle amplification, the signal would be further magnified many times,  
31  
32 98 indicating the detection system has high signal-to-noise ratio and low detection limit.

33  
34  
35  
36 99 In the past of decades, many methods have been developed to detect different targets<sup>[25]</sup>.  
37  
38  
39 100 For example, sandwich system was designed by John to detect *Campylobacter jejuni* based  
40  
41 101 on magnetic bead and quantum dot in 2009<sup>[26]</sup>, and potentiometric analysis was employed by  
42  
43 102 Gustavo to test *Escherichia coli* based on single-walled carbon nanotube in 2010<sup>[27]</sup>.  
44  
45  
46 103 Although many methods for *S. paratyphi A* detection have been developed, including  
47  
48 104 spectroscopy, PCR, antibody, immunization and gene, they have some limitations<sup>[28-30]</sup>. The  
49  
50 105 major problems of the spectroscopy methods are weak fluorescence signal and narrow  
51  
52 106 detection range. Furthermore, the use of antibody is expensive, and the procedures of PCR  
53  
54  
55 107 and immunization methods are complicated.

1  
2  
3  
4 108 In this study, a very sensitive and specific aptasensor was designed to detect *S. paratyphi A*  
5  
6 109 based on two-FAMs superposition and DNase I-mediated target recycling amplification with  
7  
8  
9 110 weak background signal. Because of fluorescence superposition by two FAM-labelled probes  
10  
11 111 and random digestion of both dsDNA and ssDNA by DNase I, less probes and aptamers are  
12  
13  
14 112 needed. Furthermore, the probes-conjugated aptasensor combined with DNase I hydrolysis  
15  
16 113 provide a lower detection limitation and higher specificity in bacteria rapid detection than  
17  
18  
19 114 previously reported methods. Cosequently, this aptasensor offers a rapid, sensitive and  
20  
21 115 specific way to detect *S. paratyphi A* and has great prospect in other pathogens'  
22  
23  
24 116 determination.

25  
26 117 .

27  
28  
29 118

30  
31 119

32  
33  
34 120

35  
36 121

37  
38  
39 122

40  
41 123

42  
43  
44 124

45  
46 125

47  
48  
49 126

50  
51 127

52  
53  
54 128

55  
56 129

1  
2  
3  
4 130 **2. Materials and methods**

5  
6 131

7  
8  
9 132 **2.1. Materials and reagents**

10  
11 133 GO was obtained from Nanjing XFNANO Materials Tech Co. Ltd (Nanjing, China). DNase I  
12  
13 134 was purchased from Thermo. Bacteria were maintained in our laboratory. The stretched  
14  
15 135 aptamer, the probe 1 and probe 2 were synthesized by Sangon Biotechnology CO. Ltd  
16  
17 136 (shanghai China). The DNA oligonucleotide sequences were listed below:

18  
19  
20  
21 137 Probe 1: 5'-TCTAGA-FAM-3'

22  
23 138 Probe 2: 5'-FAM-TCATGA-3'

24  
25  
26 139 DA: 5'-TCTAGAGCCACGCGCAGCAATCAAACCCGGCCCCCTGCTCATGA-3'

27  
28  
29 140 All these sequences were dissolved with 10mM Tris-HCl buffer (pH 7.5) that was  
30  
31 141 composed of 10mM Tris-HCl (pH 7.5), 2.5mM MgCl<sub>2</sub>, and 0.1mM CaCl<sub>2</sub>. Sterile water was  
32  
33 142 used in this assay.

34  
35  
36 143

37  
38  
39 144 **2.2. Apparatus**

40  
41 145 A LS55 fluorescence spectrophotometer (PerkinElmer, UK) was used to measure  
42  
43 146 fluorescence signals. Both excitation and emission slits were set as 10nm. The excitation  
44  
45 147 wavelength was 480nm and the emission spectra ranged from 300nm to 700nm. The  
46  
47 148 fluorescence intensity at 517nm was applied to estimate the performance of the assay. All  
48  
49 149 measurements were carried out at room temperature. Origin 8.0 software was adopted to deal  
50  
51 150 with the experimental data, and Fluorescence WinLab was used to cope with the fluorescence  
52  
53  
54  
55  
56 151 spectra.



1  
2  
3  
4 152 2.3. Preparation of GO

5  
6 153 One hundred mL sterile water was added to a conical tube containing 0.1g of GO prepared  
7  
8 154 from natural graphite by the modified Hummers method<sup>[31]</sup>. The mixture was placed in an ice  
9  
10 155 bath and homogenized ultraphonic by an ultrasonic cell disruptor at 150W for 2h before a  
11  
12 156 homogeneous GO solution was obtained and stored at room temperature for later use.  
13  
14  
15

16 157

17  
18  
19 158 2.4. Gel-electrophoresis

20  
21 159 Gel-electrophoresis was conducted to confirm the feasibility of the method. The product of  
22  
23 160 every reaction was collected. Samples for electrophoresis were prepared individually as  
24  
25 161 aptasensor, aptasensor/GO complex, aptasensor/target complex, mixture of aptasensor/target  
26  
27 162 complex (aptasensor: probe 1 plus DA plus probe 2) and DNase I, mixture of aptasensor  
28  
29 163 1/target complex (aptasensor 1: probe 1 plus DA) and DNase I, mixture of aptasensor 2/target  
30  
31 164 complex (aptasensor 2: probe 2 plus DA) and DNase I. Each was mixed with 2 $\mu$ L loading  
32  
33 165 buffer and loaded onto 4% agarose gel. The electrophoresis was performed in 10mM  
34  
35 166 Tris-HCl (pH7.5) buffer at 120V for 45min. Then the resulting gel image was photographed  
36  
37 167 under UV light.  
38  
39  
40  
41  
42  
43  
44

45 168

46 169 2.5. Determination of target by DNase I-mediated fluorescence amplification system

47  
48 170 Probe 1, probe 2 and DA were denatured at 95 $^{\circ}$ C for 5min in water bath and cooled for 10  
49  
50 171 min in ice bath. Subsequently, 25nM of them were mixed together and incubated at 25 $^{\circ}$ C for  
51  
52 172 20min. GO was then added to the mixture and incubated for 10min at 25 $^{\circ}$ C to quench the  
53  
54 173 fluorescence in the two FAM-modified terminal probes. The fluorescence values were  
55  
56  
57  
58  
59  
60

1  
2  
3  
4 174 measured after different concentrations of the bacterium were added into the mixture and  
5  
6 175 incubated at 37°C for 20min. The amplified fluorescent signals were measured after the  
7  
8  
9 176 addition of 1U DNase I to the solution for 30min at 37°C in water bath. The experiments to  
10  
11 177 optimize detection conditions were conducted under identical conditions.  
12  
13  
14 178

## 15 16 179 2.6. Specificity assay

17  
18  
19 180 Specificity assay was conducted by appending different bacteria, including *Salmonella*  
20  
21 181 *paratyphi A*, *Salmonella. cholerae-suis*, *Escherichia coli K88*, *Staphylococcus aureus* and  
22  
23  
24 182 *Bacillus thuringiensis*, to the reaction system. Bacteria ( $1 \times 10^{11}$  cells/mL) were incubated with  
25  
26 183 25nM aptasensor/GO complex for 20min in 37°C water bath, and 1U DNase I was  
27  
28  
29 184 subsequently added to the mixtures and incubated for 30min before the fluorescent intensities  
30  
31 185 were measured.  
32  
33  
34 186

## 35 36 187 2.7. Samples detection

37  
38  
39 188 Milk and water were selected as samples for bacteria detection. Different concentrations of  
40  
41 189 bacteria were added to milk and water in centrifuge tubes, respectively. The aptasensor/GO  
42  
43  
44 190 complex in working solution were mixed with various concentrations of bacteria for 20min  
45  
46 191 and subsequently incubated with 1U DNase I for 30min in 37°C water bath, and their  
47  
48  
49 192 fluorescent intensities were measured. All experiments were repeated in triplicates.  
50  
51  
52 193

## 53 54 194 3. Results and discussion

55  
56 195  
57  
58  
59  
60

1  
2  
3  
4 196 3.1. Aptamer selection and identification

5  
6 197 A group of ssDNA aptamers with high affinity and specificity against *S. paratyphi A* were  
7  
8 198 selected from an enriched oligonucleotide pool by SELEX process. Several other food-borne  
9  
10 199 bacteria were used as counter-selection targets. Through several rounds of positive-SELEX  
11  
12 200 and counter-SELEX, aptamers were sorted, cloned, sequenced, and characterized for binding  
13  
14 201 efficiency. Table 1 showed the aptamer sequences for the bacteria. The aptamer sequences  
15  
16 202 from cell-SELEX were longer than those from protein-SELEX. Taking the cost and high  
17  
18 203 binding affinity into consideration, aptamer 3 was chosen as the experiment sequence.  
19  
20  
21  
22  
23  
24

25  
26 205 3.2. Design principle

27  
28 206 Recycling amplification was used to detect many targets, such as ATP, bacterium, protein,  
29  
30 207 cell and so on. It was also vital to design a new recycling amplification aptasensor to improve  
31  
32 208 detection signal and decrease detection limit. As shown in Figure 1, DA was a sequence of  
33  
34 209 aptamer 3 flanked by six nucleotides at the 5'-terminal and four nucleotides at the 3'-terminal,  
35  
36 210 which kept a structure similar to that of the initial aptamer 3. The aptasensor, designated as  
37  
38 211 two-FAMs modified aptasensor, was composed of three segments in Figure 2. Segment 1 was  
39  
40 212 the DA, segment 2 was the probe 1 with six bases completely complementary to the  
41  
42 213 5'-terminal of DA, and segment 3 was the probe 2 with six bases completely complementary  
43  
44 214 to the 3'-terminal of DA. Unlike the traditional quenching agents, GO was widely used  
45  
46 215 because of its high quenching rate, low cost and excellent bio-compatibility. In the absence of  
47  
48 216 target, the aptasensor was hybridized with GO by  $\pi$ - $\pi$  stacking and the fluorophore of FAM  
49  
50 217 was weak due to GO quenching based on fluorescence resonance energy transfer (FRET).  
51  
52  
53  
54  
55  
56  
57  
58  
59  
60

1  
2  
3  
4 218 When target was introduced, however, the aptasensor dissociated from GO due to specific  
5  
6 219 recognition and binding of the aptasensor with the target, resulting in the recovery of  
7  
8  
9 220 fluorescence. Importantly, the fluorescent signal was significantly amplified by DNase  
10  
11 221 I-mediated target recycle process in which all DNA sequences were degraded by DNase I,  
12  
13 222 leading to release of target and FAM fluorophores, and the released target was recycled  
14  
15 223 repeatedly, leading to accumulation of free FAM fluorophores.  
16  
17  
18  
19 224

20  
21 225 To further investigate the feasibility of rapid bacterial detection, fluorescence emission  
22  
23 226 spectra of the aptasensor were analysed under various conditions. As shown in Figure 3, the  
24  
25 227 fluorescence spectrum ( $f_0$ ) of the aptasensor showed the highest intensity (curve a), whereas  
26  
27 228 more than 97% fluorescence was quenched when appropriate amount of GO was added into  
28  
29 229 the system (curve b), suggesting that aptasensor/GO complex was formed so that GO could  
30  
31 230 quench the FAM fluorescence efficiently. When DNase I was added to aptasensor/GO  
32  
33 231 complex, the fluorescence intensity did not increase obviously (curve c), revealing that the  
34  
35 232 aptasensor was completely inserted in GO and protected from being digested by DNase I.  
36  
37 233 Interestingly, the fluorescence intensities were raised dramatically upon the addition of target  
38  
39 234 (curve d), and elevated to 70% of  $f_0$  upon the addition of target plus DNase I (curve e),  
40  
41 235 demonstrating that the aptasensor was released from GO by its specific binding to target and  
42  
43 236 so the FAM fluorescence was no longer quenched, and that DNase I amplified the fluorescent  
44  
45 237 signal by randomly digesting single- and double-stranded sequences of DNA in the presence  
46  
47 238 of  $Mg^{2+}$  and therefore triggering the target recycling process, generating more free FAM  
48  
49 239 fluorophores. Specifically, the fluorescence emission spectra of both aptasensor 1/target  
50  
51  
52  
53  
54  
55  
56  
57  
58  
59  
60

1  
2  
3  
4 240 complex and aptasensor 2/target complex were also depicted through the DNase I-mediated  
5  
6 241 target recycling process (curve f and g, respectively). Comparing with the fluorescent  
7  
8  
9 242 intensities of the aptasensor in the absence and presence of DNase I-mediated target recycling  
10  
11 243 (curve d and e, respectively), neither the aptasensor 1/target complex nor the aptasensor  
12  
13 244 2/target complex showed stronger fluorescence intensity than the aptasensor system.  
14  
15  
16 245 Consequently, the bacteria could be quickly detected through aptamer recognition and DNase  
17  
18  
19 246 I signal amplification.

20  
21 247 In order to verify the superiority of the two-FAMs modified aptasensor over the one-FAM  
22  
23 248 modified ones, the fluorescent intensities between one-FAM modified aptasensors  
24  
25 249 (aptasensor 1 and 2) and the aptasensor were compared as well. These data under different  
26  
27 250 conditions were shown in Supplementary Information Figure 1S. The fluorescent recovery  
28  
29 251 rates of aptasensor 1 and 2 were 34% and 27% in the absence of DNase I, 53% and 40% in  
30  
31 252 the event of 1U DNase I, which were 13% - 20% and 17% - 30% lower than those of the  
32  
33 253 aptasensor. Because it has high fluorescence intensities and fluorescent recovery, the  
34  
35 254 aptasensor with high fluorescence intensity and fluorescent recovery exhibited more  
36  
37 255 favorable feasibility.  
38  
39  
40  
41  
42  
43  
44  
45

### 46 257 3.3. Optimization of test conditions

47  
48 258 To optimize the detection platform, the concentration and reaction time of GO, the reaction  
49  
50 259 time of target and DNase I were required further experiment. Because the ratio of  
51  
52 260 nanomaterial and biomolecule is a critical factor in the detection system, it is essential to  
53  
54 261 investigate the proper ratio between DA and GO. Nine different GO concentrations (from 0 to  
55  
56  
57  
58  
59  
60

1  
2  
3  
4 262 80µg/mL) were prepared and incubated with 25nM aptasensors (25nM aptasensor: 25nM  
5  
6 263 probe 1 plus 25nM DA plus 25nM probe 2; 25nM aptasensor 1: 25nM probe 1 plus 25nM  
7  
8 264 DA; 25nM aptasensor 2: 25nM DA plus 25nM probe 2) in 25°C water bath for 10min,  
9  
10  
11 265 respectively. Their fluorescence intensities were measured at 517nm with the excitation at  
12  
13 266 480nm. As displayed in Figure 4A, the fluorescence intensity decreased with an increase in  
14  
15  
16 267 GO concentration. When GO concentration reached 60µg/mL, the fluorescence intensities  
17  
18 268 were quenched by 97% for 25nM aptasensor and by 95% for 25nM aptasensor 1 and 2,  
19  
20  
21 269 indicating that 60µg/mL was the saturation point to quench 25nM aptasensors and thus  
22  
23  
24 270 applied to the subsequent experiments.

25  
26 271 To determine the optimal incubation time of GO, target and DNase I, fluorescence  
27  
28 272 intensities were tested every 5min with a reaction solution (25nM aptasensor, 60µg/mL GO,  
29  
30  
31 273  $1 \times 10^{11}$  cells/mL bacteria, 1U DNase I in Tris-HCl buffer), respectively. When GO was  
32  
33  
34 274 incubated with the aptasensor at 25°C for 10min, the fluorescence intensity reached the  
35  
36 275 saturation point (Figure 4B). Thus 10min was selected as the optimal incubation time of GO.  
37  
38 276 With the addition of target, the fluorescence intensity increased with time. As it increased  
39  
40  
41 277 quickly in 20min and slowly from 20min to 60min, 20min was chosen for the optimal  
42  
43  
44 278 incubation time of target. Likewise, 30min was supposed as the effective incubation time of  
45  
46 279 DNase I.

47  
48  
49 280

### 50 51 281 3.4. Electrophoresis characterization

52  
53  
54 282 To confirm the feasibility of this method, agarose gel electrophoresis was done. As displayed  
55  
56 283 in Figure 5, DNA marker had nine bands (lane 1). The aptasensor presented only one bright  
57  
58  
59  
60

1  
2  
3  
4 284 band between 50bp and 25bp after 45min at 60V/cm (lane 2), indicating the aptasensor was  
5  
6 285 established successfully in the reaction buffer. No band was observed with the addition of GO  
7  
8  
9 286 (lane 3), demonstrating that aptasensor was bound to GO, and no free probe was supposed to  
10  
11 287 exist in buffer. Whereas a bright band appeared again after target was added into the buffer  
12  
13 288 (lane 4), suggesting that the aptasensor was pulled off from GO due to its specific binding to  
14  
15  
16 289 target, and the affinity between the aptasensor and target was stronger than  $\pi$ - $\pi$  stacking.  
17  
18  
19 290 However, no band was displayed when DNase I was added (lane 5), indicating that the  
20  
21 291 aptasensor was completely digested by the enzyme into mono- and oligodeoxyribonucleotides.  
22  
23 292 Similarly, when the samples of DNase I-treated aptasensor 1/target complex and aptasensor  
24  
25 293 2/target complex were loaded, no bands were seen (lane 6 and lane 7), confirming the  
26  
27  
28 294 successful digestion of aptasensors by DNase I. As a result, our method proved effective and  
29  
30  
31 295 feasible.

32  
33  
34 296

### 35 36 297 3.5. Sensitivity of the aptasensor

37  
38  
39 298 In order to explore its sensitivity, which was an important factor for biosensor, parallel assays  
40  
41 299 were performed. Gradient concentrations of target (from  $10^3$  to  $10^{11}$  cells/mL) were prepared  
42  
43  
44 300 and mixed with the reaction solution which contained aptasensor/GO complex, and the  
45  
46 301 fluorescence emission spectra were recorded. As depicted in Figure 6A, their fluorescence  
47  
48  
49 302 intensities were recovered after the addition of target and exhibited a remarkable increasing  
50  
51 303 tendency from  $10^3$  to  $10^{11}$  cells/mL. The linear correlation was  $Y = 44.269x - 100.399$ , where  
52  
53  
54 304 Y was the fluorescence intensity and X was the concentration of the bacterium in logarithmic  
55  
56 305 phase, respectively (regression coefficient  $R^2 = 0.99340$ ). The results indicated that the  
57  
58  
59  
60

1  
2  
3  
4 306 addition of target led to formation of the aptasensor/target complex and contributed to release  
5  
6 307 of the fluorophores from GO, and the detection sensitivity of this method were improved  
7  
8  
9 308 greatly via fluorescence superposition .

10  
11 309

### 12 13 14 310 3.6. Signal amplification by DNase I

15  
16 311 To achieve signal amplification DNase I was exploited to the system. Ten  $\mu\text{L}$  of 10U DNase I  
17  
18 312 was added to 100 $\mu\text{L}$  reaction solution and incubated with aptasensor/target complex in 37°C  
19  
20  
21 313 water bath for 30min. Greater fluorescent signal and lower detection limit ( $1 \times 10^2$  cells/mL)  
22  
23  
24 314 were obtained with the addition of both target and DNase I (Figure 6A, 6B). Moreover, a  
25  
26 315 good linear relation was located from  $1 \times 10^2$  to  $1 \times 10^{11}$  cells/mL ( $Y = 45.186x - 35.824$ ,  $R^2 =$   
27  
28 316 0.99802). The results displayed that the signal amplification was really achieved by the  
29  
30  
31 317 DNase I-mediated target recycling reaction.

32  
33  
34 318

### 35 36 319 3.7. Specificity of the aptasensor

37  
38  
39 320 To evaluate the specificity of the system which was another important factor of aptasensor,  
40  
41 321 parallel assays were done. The controls, including *S. cholerae-suis*, *E. coli K88*, *S. aureus*, *B.*  
42  
43 322 *thuringiensis*, were incubated with the aptasensor/GO complex and DNase I, respectively.  
44  
45  
46 323 Their fluorescence emission spectra were measured. As shown in Figure 7, the fluorescence  
47  
48  
49 324 intensities of target were much stronger than those of the controls. The results demonstrated  
50  
51 325 that the method could distinguish the target from the controls with high specificity. Meanwhile,  
52  
53  
54 326 the aptasensor remained the specificity of aptamer 3 and could identify its target effectively.  
55  
56 327 Therefore, we believe that the aptasensor in our study are highly selective for target and it is a  
57  
58  
59  
60



1  
2  
3  
4 328 promising method for the detection of samples with complicated matrix.  
5  
6  
7 329

8  
9 330 **3.8. Application for samples**

10  
11 331 In order to test the application of this system in real samples, we determined some bacteria in  
12  
13 332 milk and water. As observed in Figure 8, their fluorescence intensities were between the  
14  
15 333 aptasensor and aptasensor/GO complex when various bacteria in samples were detected by  
16  
17 334 this method. However, the fluorescence emission spectra of non-target bacteria detection  
18  
19 335 were lower than those of target. The observed results demonstrated well that the established  
20  
21 336 method is competent in real samples detection.  
22  
23  
24  
25  
26  
27 337

28  
29 338 **Conclusions**

30  
31 339 In this study, we have successfully developed a simple, highly selective and sensitive  
32  
33 340 aptasensor for *Salmonella paratyphi A* detection by using GO as an efficient fluorescence  
34  
35 341 quencher and DNase I as a competent signal amplifier. As it can detect target with a wide  
36  
37 342 linear range (from  $1 \times 10^2$  to  $1 \times 10^{11}$  cells/mL) and a low detection limit ( $1 \times 10^2$  cells/mL), the  
38  
39 343 aptasensor is superior to other methods ( $10^6$  cells/mL detected by spectrophotometry and  $10^5$   
40  
41 344 cells/mL by fluorescence). More importantly, its operational process is simpler than them,  
42  
43 345 that require extraction of specific genes (iroB and gyrA gene) or use complex multi-enzymes  
44  
45 346 (exonuclease I and exonuclease III). GO employed in this system has its intrinsic advantages  
46  
47 347 over other materials, such as low cost, high quenching efficiency, homogeneous dispersibility  
48  
49 348 and so on. In addition, significant fluorescence signals can be attained with high sensitivity  
50  
51 349 and specificity when this aptasensor is adopted to test target in samples. DNase I was first  
52  
53  
54  
55  
56  
57  
58  
59  
60

1  
2  
3  
4 350 used for bacteria detection based on its unique properties of digesting dsDNA and ssDNA  
5  
6 351 randomly and simultaneously, resulting in degradation of aptasensor from fluorophore-  
7  
8  
9 352 aptasensor/target complex and release of target and fluorophore. Also, the target recycling  
10  
11 353 makes it possible to release more fluorophores and hence to achieve an amplified  
12  
13 354 fluorescencet signal. Furthermore, the two-fluorophore aptasensor produces higher  
14  
15  
16 355 fluorescence intensity than the one-fluorophore aptasensor in this system. Meanwhile, its  
17  
18  
19 356 quantity is small and fluorescence intensity upbeat. Consequently, the aptasensor should be  
20  
21 357 considered as a new tool for other sample detections since it has high sensitivity and  
22  
23  
24 358 specificity.  
25  
26  
27  
28

## 29 360 **Acknowledgments**

30  
31 361 We would like to thank National Natural Science Foundation (81271660), the Specialized  
32  
33 362 Research Fund from the Ministry of Education for the Doctoral Program of Higher Education  
34  
35  
36 363 (20114306110006) and Hunan Provincial Key Laboratory Open Foundation for Microbial  
37  
38  
39 364 Molecular Biology (2014-01) for financial support.  
40  
41  
42  
43  
44 365  
45  
46 366  
47  
48  
49 367  
50  
51 368  
52  
53 369  
54  
55 370  
56  
57 371  
58  
59 372  
60

373 **References**

- 374 1. L.P. Forshell, M. Wierup, *Rev. Sci. Tech.*, 2006, 25, 541-554.
- 375 2. M.I. Khan, S.M. Sahito, M.J. Khan, S.M. Wassan, A.W. Shaikh, M.A. Kaheshwari, C.J.  
376 Acosta, C.M. Galindo, R.L. Ochiai, S. Rasool, S. Peerwani, M.K. Puri, M. Ali, A. Zafar, R.  
377 Hassan, L. von Seidlein, J.D. Clemens, S.Q. Nizami, Z.A. Bhutta, *Bull World Health*  
378 *Organ.*, 2006, 84, 72-77.
- 379 3. C.S. Teh, K.H. Chua, K.L. Thong, *Int. J. Med. Sci.*, 2014, 11, 732-741.
- 380 4. V. Ganesan, B.N. Harish, G.A. Menezes, S.C. Parija, *J Clin. Diagn. Res.*, 2014, 8,  
381 DC01-03.
- 382 5. M.N. Widjojatmodjo, A.C. Fluit, R. Torensma, B.H. Keller, J. Verhoef, *Eur. J. Clin.*  
383 *Microbiol. Infect. Dis.*, 1991, 10, 935-938.
- 384 6. W. Chen, G. Martinea, A. Mulchandani, 2000, 280, 166-172.
- 385 7. A. Caballero, M.J. García-Pereira, H. Quesada, *BMC Genomics*, 2013, 14, 528.
- 386 8. M. Yüce, N. Ullah, H. Budak, *Analyst*, 2015, 140, 5379-5399.
- 387 9. S. Korbsrisate, S. Sarasombath, N. Praaporn, P. Iamkamala, M. Hossain, S. Mckay,  
388 *Southeast Asian J. Trop Med. Public Health*, 1998, 29, 864-871.
- 389 10. G.Q. Liu, X.F. Yu, W. Chen, F. Xue, Y.K. Ye, X.J. Yang, Y.Q. Lian, Y. Yan, K. Zong.  
390 *Microchim. Acta.*, 2012, 178, 237-244.
- 391 11. Z.J. Li, Y. Song, W.H. Zhu, L. Deng, *Anal. Methods*, 2015, 7, 970-975.
- 392 12. H.X. Chang, L.H. Tang, Y. Wang, J.H. Jiang, J.H. Li, *Anal. Chem.*, 2010, 82, 2341-2346.
- 393 13. A. Ganji, A. Varasteh, M. Sankian, *J. Drug Target*, 2015, 7, 1-12.
- 394 14. Z.S. Qian, X.Y. Shan, L.J. Chai, *Biosens. Bioelectron*, 2015, 68, 225-231.

- 1  
2  
3  
4 395 15. C. Liu, G.B. Mao, C. Su, X.H. Ji, Z.L. Chen, Z.K. He, *Anal. Methods*, 2015, DOI:  
5  
6 396 10.1039/C5AY01728A.  
7  
8  
9 397 16. J.G. Bruno, *Molecules*, 2015, 20, 6866-6887.  
10  
11 398 17. H. Sun, Y. Zu, *Molecules*, 2015, 20, 11959-11980.  
12  
13 399 18. Y. Xie, X. Lin, Y. Huang, R. Pan, Z. Zhu, L. Zhou, C.J. Yang, *Chem. Commun.*, 2015, 51,  
14  
15 400 2156-2158.  
16  
17  
18 401 19. J.M. Liu, X.P. Yan, *Biosens. Bioelectron.*, 36, 2012, 135-141.  
19  
20  
21 402 20. A. Benvidi, A.D. Firouzabadi, S.M. Moshtaghiun, M. Mazloum-Ardakani, M.D. Tezerjani,  
22  
23 403 *Anal. Biochem.*, 2015, 484, 24-30.  
24  
25  
26 404 21. Y.X. Xu, H. Bai, G.W. Lu, C. Li, G.Q. Shi, *J. Am. Chem. Soc.*, 2008, 130, 5856-5857.  
27  
28  
29 405 22. Y. Zhang, W. Liu, C.E. Banks, F. Liu, M. Li, F. Xia, X. Yang, *Sci. Rep.*, 2014, 4:7556,  
30  
31 406 DOI: 10.1038/srep07556.  
32  
33  
34 407 23. Y. Ning, W. Li, Y. Duan, M. Yang, L. Deng, *J. Biomol. Screen*, 2014, 19, 1099-1106.  
35  
36  
37 408 24. M. Yang, Z. Peng, Y. Ning, Y. Chen, Q. Zhou, L. Deng, *Sensors*, 2013, 13, 6865-6881.  
38  
39  
40 409 25. M. Abdolrahim, M. Rabiee, S.N. Alhosseini, M. Tahriri, S. Yazdanpanah, L. Tayebi.  
41  
42 410 *Anal. Biochem.*, 2015, 485, 1-10.  
43  
44 411 26. J.G. Bruno, T. Phillips, M.P. Carrillo, R. Crowell, *J. Fluoresc.*, 2009, 19, 427-435.  
45  
46 412 27. G.A. Zelada-Guillén, S.V. Bhosale, J. Riu, F.X. Rius, *Anal. Chem.* 2010, 82, 9254-9260.  
47  
48  
49 413 28. G.J. Ngan, L.M. Ng, R.T. Lin, J.W. Teo, *Res. Microbiol.*, 2010, 161, 243-248.  
50  
51  
52 414 29. S. Korbsrisate, S. Sarasombath, K. Janyapoon, P. Ekpo, S. Pongsunk, *Appl. Environ.*  
53  
54 415 *Microbiol.*, 1994, 60, 4612-4613.  
55  
56 416 30. T. Dimitrov, A.A. Dashti, O. Albaksami, M.M. Jadaon, *J. Clin. Pathol.*, 2010, 63, 83-87.  
57  
58  
59  
60

1  
2  
3  
4 417 31. J.G. Moo, B. Khezri, R.D. Webster, M. Pumera. Chemphyschem., 2014, 15, 2922-2929.

5  
6 418

7  
8  
9 419 **Footnotes**

10  
11 420 <sup>1</sup>This work was financially supported by the National Natural Science Foundation  
12  
13 421 (81271660), the Specialized Research Fund from the Ministry of Education for the Doctoral  
14  
15 422 Program of Higher Education (20114306110006) and Hunan Provincial Key Laboratory  
16  
17 423 Open Foundation for Microbial Molecular Biology (2014-01).

18  
19 424 <sup>2</sup>Abbreviations usage: DA, designed aptamer; FRET, fluorescence resonance energy transfer;  
20  
21 425 GO, graphene oxide; DNase I, deoxyribonuclease I; FAM, carboxyfluorescein; SELEX,  
22  
23 426 systematic evolution of ligands by exponential enrichment; ssDNA, single-stranded DNA;  
24  
25 427 dsDNA, double-stranded DNA; *S. paratyphi A*, *Salmonella paratyphi A* (isolated from  
26  
27 428 patients infected with *Salmonella*); *S. aureus*, *Staphylococcus aureus* (ATCC25923); *S.*  
28  
29 429 *cholerae-suis*, *Salmonella cholerae-suis* (ATCC10708); *B. thuringiensis*, *Bacillus*  
30  
31 430 *thuringiensis* (CCTCC200016); *E. coli K88*, *Escherichia coli K88* (CVCC216); PCR,  
32  
33 431 Polymerase Chain Reaction; AFLP, Amplified Fragment Length Polymorphism. ATP,  
34  
35 432 adenosine triphosphate.

36  
37 433

38  
39 434

40  
41 435

42  
43 436

44  
45 437

46  
47 438

439

Table 1.

Selected Types	Aptamer Agents	Sequence (from 5' to 3')	K <sub>d</sub> [nM]
Cell-SELEX	Apt 10	GATGATGGACGTATATCGTCTCCCATGAATTCAGTCGGACAGCG	73±9
	Apt 22	ATGGACGAATATCGTCTCCCAGTGAATTCAGTCGGACAGCG	47±3
	Apt 45	ATGGACGAATATCGTCTCCCAGTGAATTCAGTCGGACAGCG	68±6
	Apt 60	CGCCACCCATAATGGATCAGGGCGGGCACCACGATG	56±9
Protein-SELEX	Apt 1	CGAAGGGGCTATGCCGCTACATAGACCGTCACGA	49±6
	Apt 2	GGCCGGCAATACGGCCGAGCCCGGGGTTCTCCGA	61±7
	Apt 3	GCCACGCGCAGCAATCAAACCCGGCCCCCTGCTCC	27±5
	Apt 4	TGGCCAGAGTACGAGTAAGGGAGGTCACAACCTTA	65±9

440

441

442

443

444

445

446

447

448

449

450

451

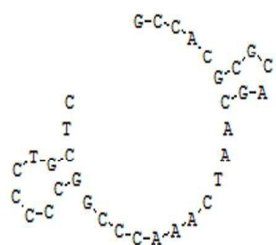
452

453

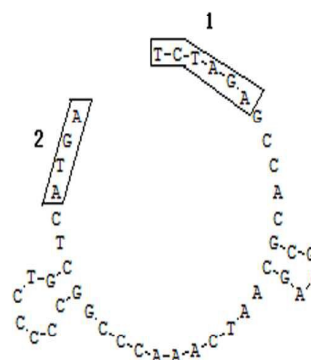
454

455

Aptamer 3



DA



456

457

Figure 1.

458

459

460

461

462

463

464

465

466

467

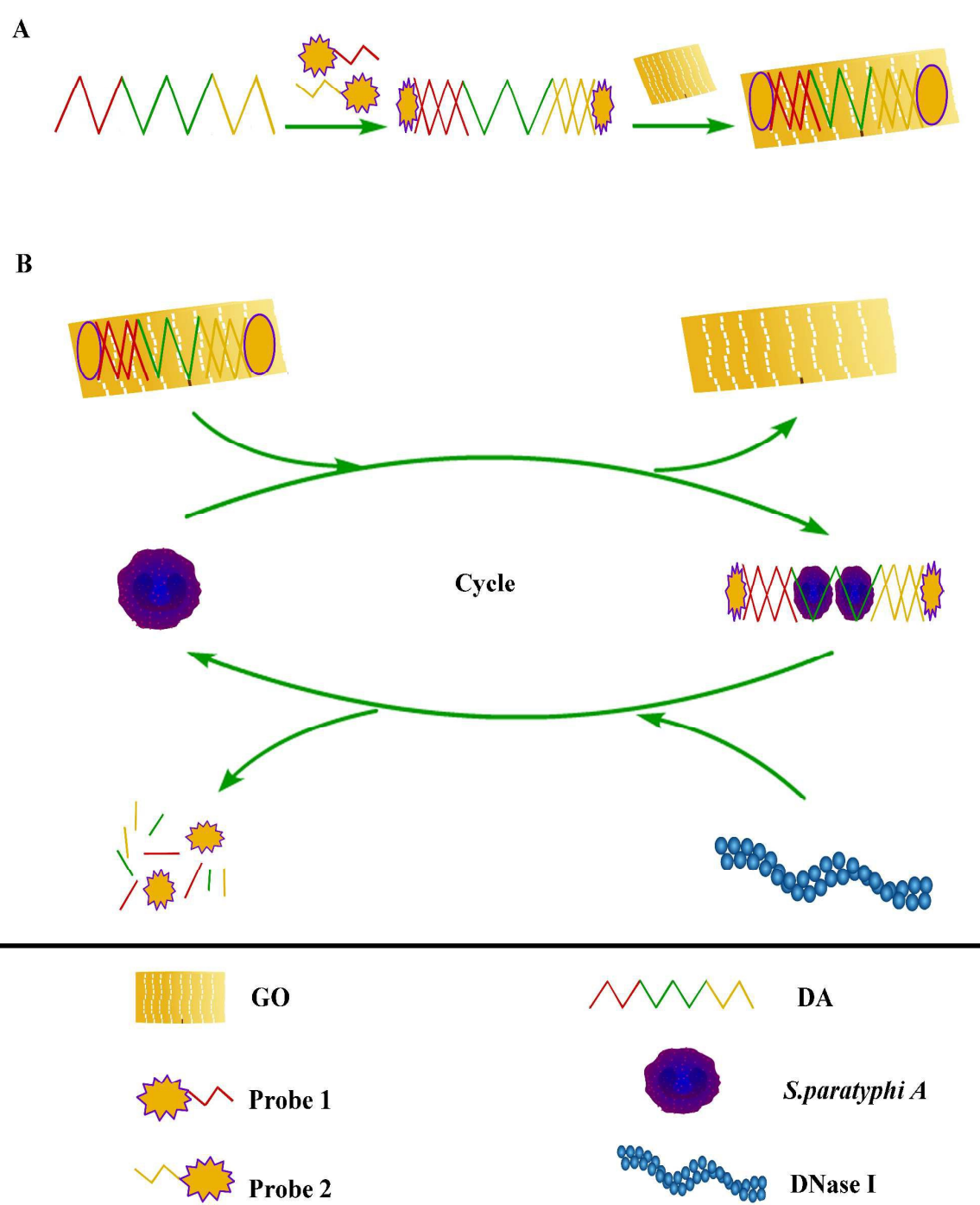


Figure 2.

468

469

470

471

1  
2  
3  
4  
5  
6  
7  
8  
9  
10  
11  
12  
13  
14  
15  
16  
17  
18  
19  
20  
21  
22  
23  
24  
25  
26  
27  
28  
29  
30  
31  
32  
33  
34  
35  
36  
37  
38  
39  
40  
41  
42  
43  
44  
45  
46  
47  
48  
49  
50  
51  
52  
53  
54  
55  
56  
57  
58  
59  
60



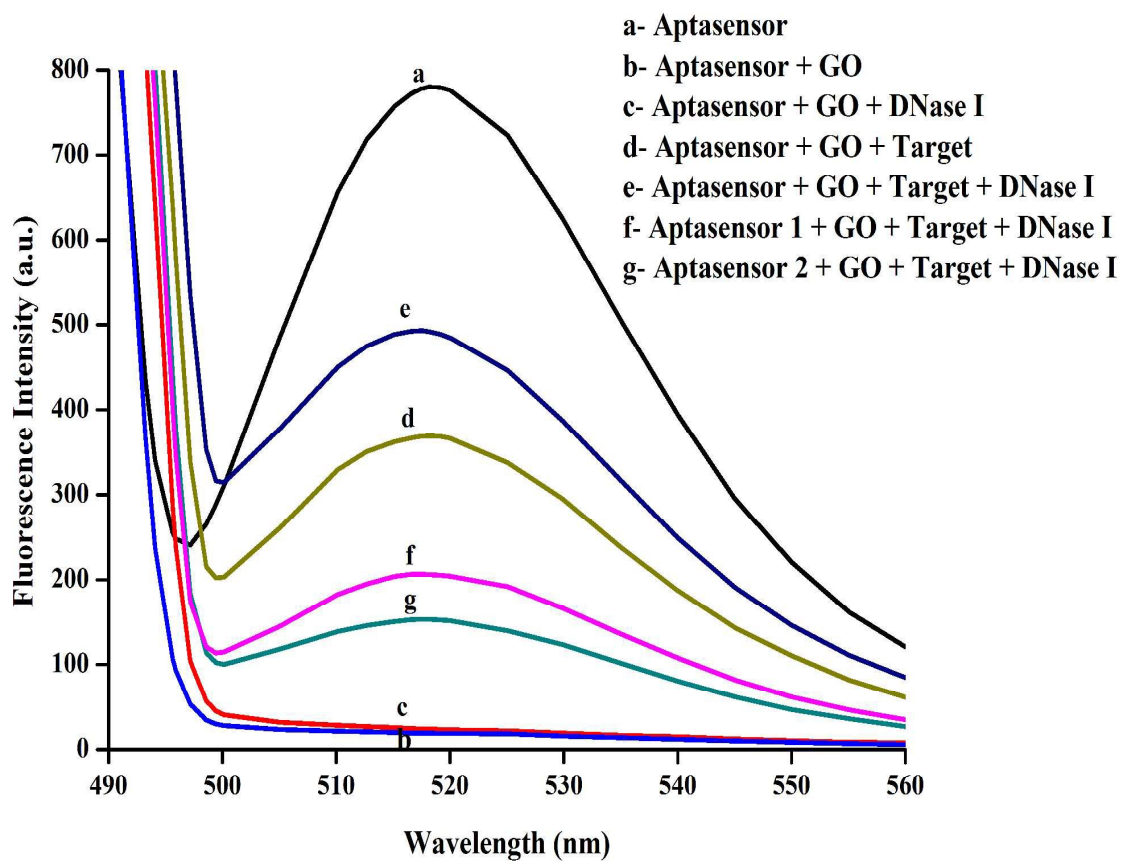
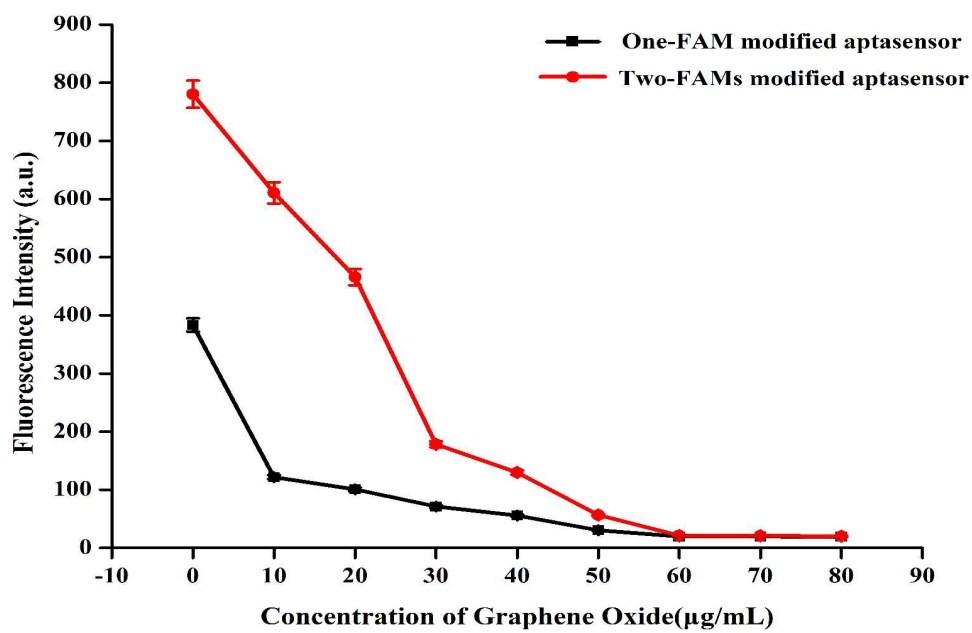


Figure 3.

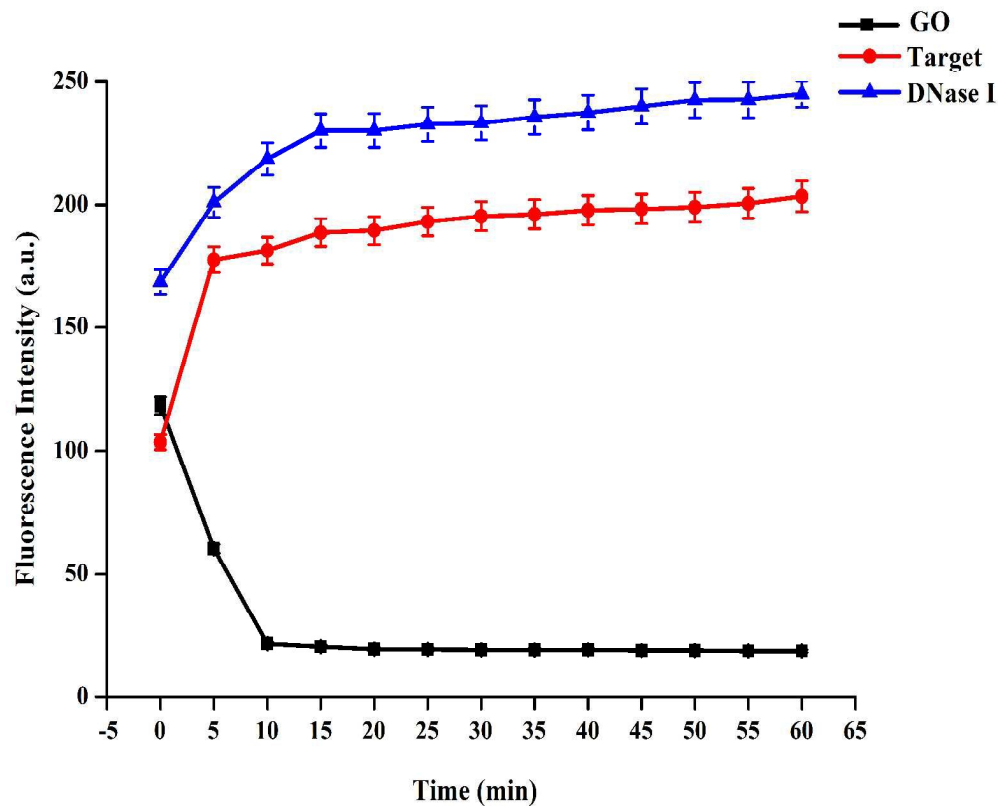
484

A



485

B

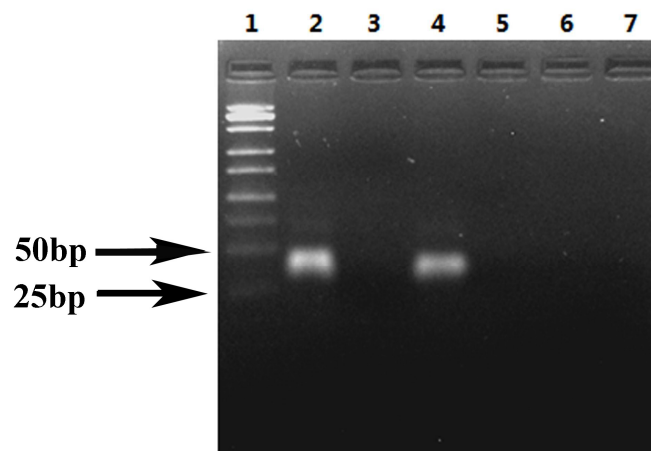


486

487

Figure 4.

488



489

490

Figure 5.

491

492

493

494

495

496

497

498

499

500

501

502

503

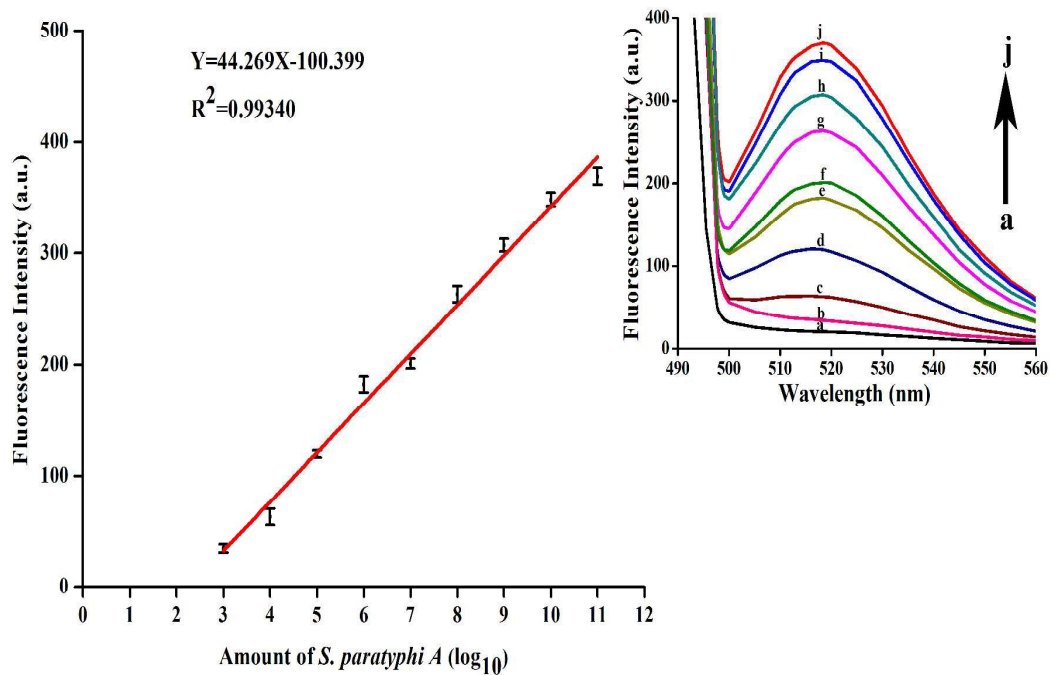
504

505

1  
2  
3  
4  
5  
6  
7  
8  
9  
10  
11  
12  
13  
14  
15  
16  
17  
18  
19  
20  
21  
22  
23  
24  
25  
26  
27  
28  
29  
30  
31  
32  
33  
34  
35  
36  
37  
38  
39  
40  
41  
42  
43  
44  
45  
46  
47  
48  
49  
50  
51  
52  
53  
54  
55  
56  
57  
58  
59  
60

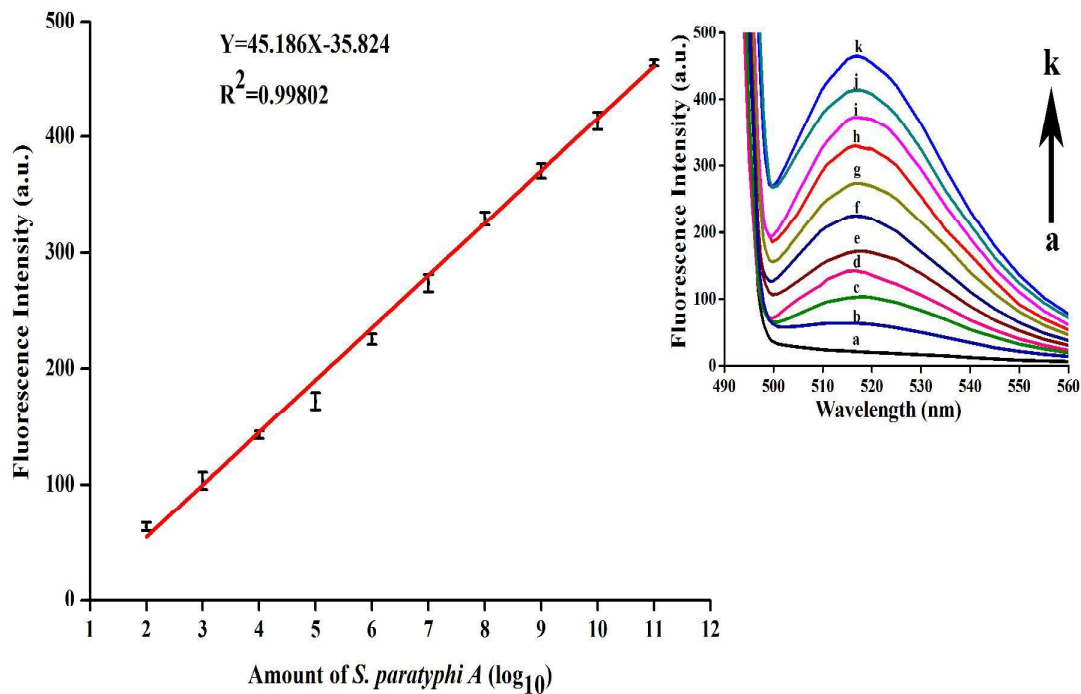
503

A



504

B



505

506

Figure 6.

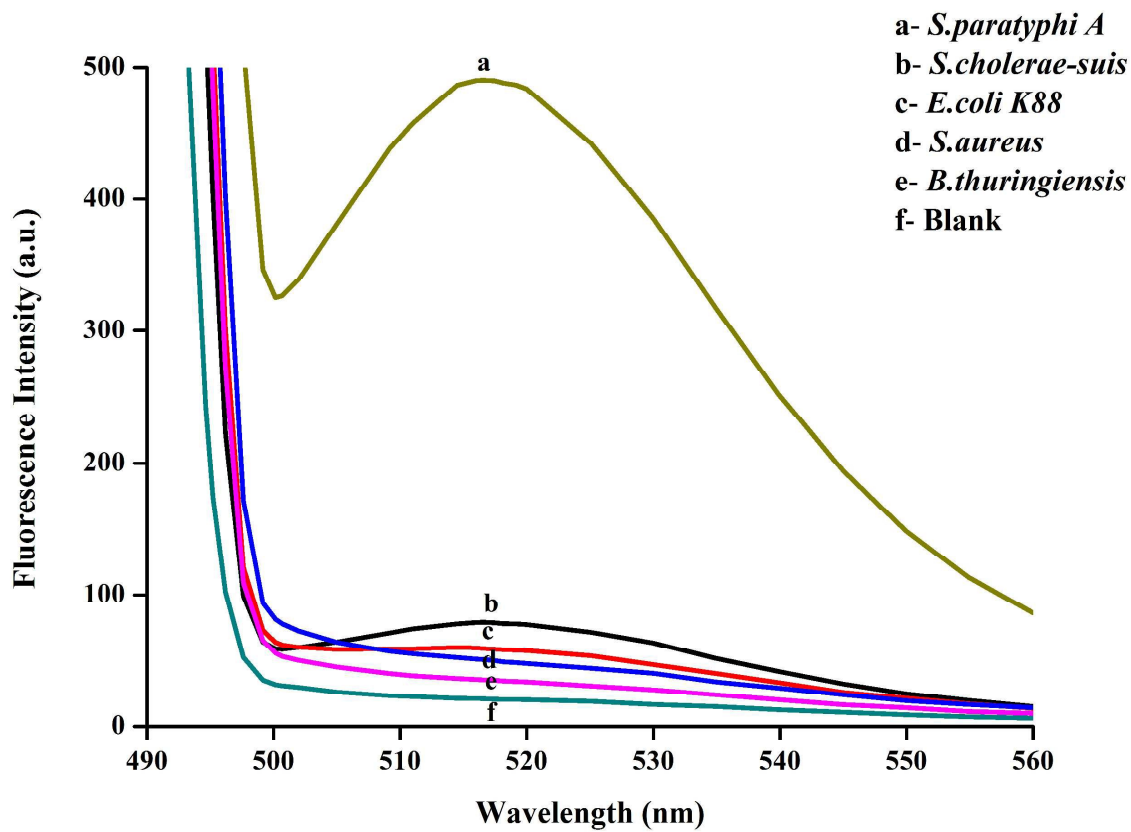


Figure 7.

519

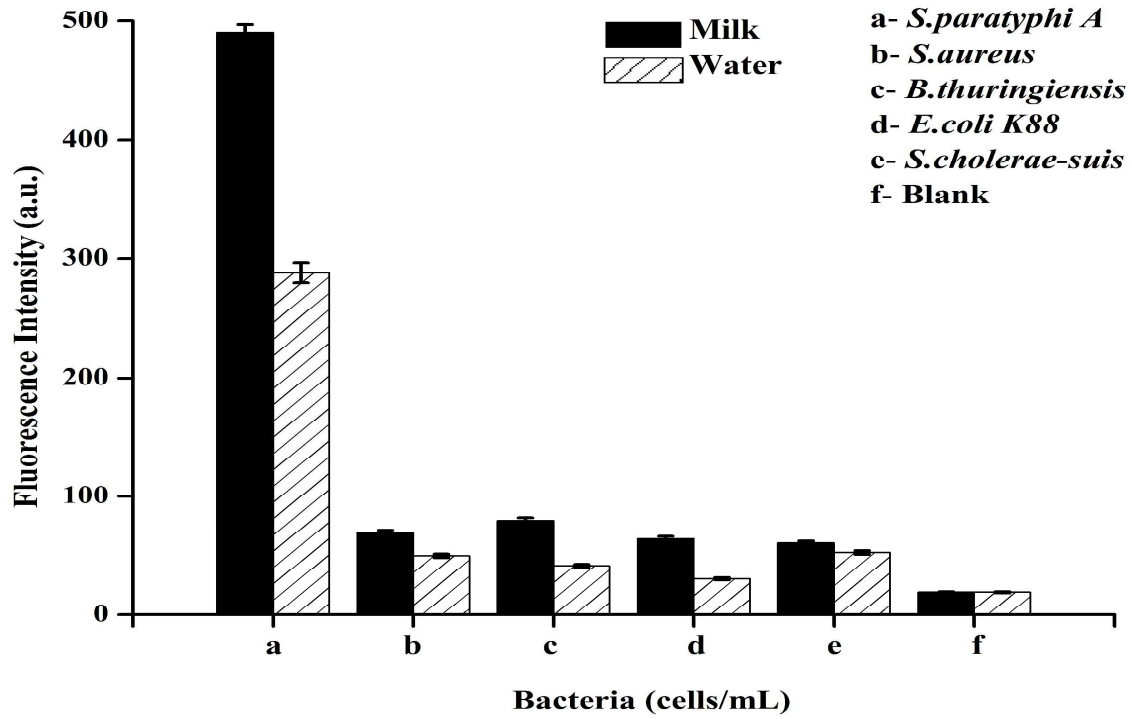


Figure 8.

520

521

522

523

524

525

526

527

528

529

530

531

532

533

534 **Captions for figures**

535 **Table 1.** Eight aptamers of *S.paratyphi A* from two types of SELEX.

536 **Figure 1.** Predicted secondary structures of the selected aptamer 3 and DA using DNAMAN  
537 software. Their minimum free energy are -2.69 kilocalorie/mol. Part 1 stands for the  
538 outstretched sequence of the aptamer 3 at 5'-end and Part 2 stands for the outstretched  
539 sequence of aptamer 3 at 3'-end in DA.

540 **Figure 2.** Schematic presentation of the detection system via GO-dependent nanoquencher  
541 and DNase I-mediated target cyclic amplification. (A) Constructions of the aptasensor and  
542 quenching effect of GO. Probe 1 and 2 combine with the DA's terminals by base  
543 complementary pairing rule accordingly. Adding GO (60µg/mL) to the reaction solution lead  
544 to quenching of fluorescence. (B) Target contributes to the recovered fluorescence and  
545 DNase I do to the amplified fluorescence further.

546 **Figure 3.** The feasibility of the proposed aptasensor. Fluorescence intensities obtained from  
547 the "product" at different stages: the initial fluorescence intensity of the aptasensor (curve a);  
548 aptasensor/GO complex (curve b); aptasensor/GO complex + DNase I (curve c); aptasensor/  
549 GO complex + target (curve d); aptasensor/GO complex + target + DNase I (curve e);  
550 aptasensor 1/GO complex + target + DNase I (curve f); aptasensor 2/GO complex + target +  
551 DNase I (curve g). The aptasensor components: 25nM DA, 25nM probe 1, 25nM probe 2.  
552 The aptasensor 1 components: 25nM DA, 25nM probe 1. The aptasensor 2 components:  
553 25nM DA, 25nM probe 2. GO concentration: 60µg/mL. Target concentration:  $1 \times 10^{11}$   
554 cells/mL. DNase I concentration: 1U.  $\lambda_{em} = 517\text{nm}$  and  $\lambda_{ex} = 480\text{nm}$ .

555 **Figure 4.** (A) The fluorescence quenching effect of GO at different concentrations. The  
556 one-FAM modified aptasensors' components: 25nM DA, 25nM probe 1 or 25nM probe 2.  
557 The two-FAMs aptasensor components: 25nM DA, 25nM probe 1 and 25nM probe 2. (B)  
558 Optimization of the reaction time for aptasensor/GO complex (solid square),

1  
2  
3 559 aptasensor/target complex (solid diamond), aptasensor/target complex + DNase I (solid  
4  
5 560 triangle). The fluorescence spectra measured at 5min time intervals in 10mM Tris-HCl  
6  
7 561 (pH7.5) buffer. GO concentration: 60 $\mu$ g/mL. Target concentration: 1 $\times$ 10<sup>7</sup> cells/mL. DNase I  
8  
9  
10 562 concentration: 1U. Error bars indicate standard deviation (n = 3).

11 563 **Figure 5.** Native polyacrylamide gel electrophoresis analysis of the “product” at different  
12  
13 564 stages: the DNA ladder (lane 1); the aptasensor (lane 2); aptasensor/GO complex (lane 3);  
14  
15 565 aptasensor/GO complex + target (lane 4); aptasensor/GO complex + target + DNase I (lane 5);  
16  
17 566 aptasensor 1/GO complex + target + DNase I (lane 6); aptasensor 2/GO complex + target +  
18  
19 567 DNase I (lane 7).

20  
21  
22  
23 568 **Figure 6.** (A) The target detection at different concentrations without DNase I. The  
24  
25 569 fluorescence intensities depend on the *S. paratyphi A* concentrations ranging from 10<sup>3</sup> to 10<sup>11</sup>  
26  
27 570 cells/mL. Fluorescence intensities in target detection: fluorescence spectral response of  
28  
29 571 aptasensor/GO complex (curve a); fluorescence emission spectra after aptasensor/GO  
30  
31 572 complex incubated with different concentrations of target (curves b to j correspond to the  
32  
33 573 concentrations ranging from 10<sup>3</sup> to 10<sup>11</sup> cells/mL). (B) The target detection at different  
34  
35 574 concentrations with DNase I. Fluorescence intensities depend on the *S. paratyphi A*  
36  
37 575 concentrations ranging from 10<sup>2</sup> to 10<sup>11</sup> cells/mL. Fluorescence intensities in target detection:  
38  
39 576 fluorescence spectral response of aptasensor/GO complex (curve a); the fluorescence  
40  
41 577 emission spectra after aptasensor/GO complex incubated with different concentrations of  
42  
43 578 target and 1U DNase I (curves b to k correspond to the concentrations ranging from 10<sup>2</sup> to  
44  
45 579 10<sup>11</sup> cells/mL). The aptasensor components: 25nM DA, 25nM probe 1, 25nM probe 2. GO  
46  
47 580 concentration: 60 $\mu$ g/mL. DNase I concentration: 1U.  $\lambda_{em}$  = 517nm and  $\lambda_{ex}$  = 480nm. Error  
48  
49 581 bars indicate standard deviation (n = 3).

50  
51  
52 582 **Figure 7.** The detection specificity of the proposed aptasensor. The concentrations of target  
53  
54 583 and other nonspecific targets were 1 $\times$ 10<sup>11</sup> cells/mL, respectively. The aptasensor components:



1  
2  
3 584 25nM DA, 25nM probe 1, 25nM probe 2. GO concentration: 60 $\mu$ g/mL. DNase I  
4  
5 585 concentration: 1U. The fluorescence intensities were read at  $\lambda_{em} = 517$ nm and  $\lambda_{ex} = 480$ nm.  
6  
7 586 Error bars indicate standard deviation (n = 3).  
8

9  
10 587 **Figure 8.** Ability verification of the approach to detect samples. Fluorescence emission  
11 588 spectra of different bacteria at the  $1 \times 10^{11}$  cells/mL in milk (solid) and the  $1 \times 10^7$  cells/mL in  
12  
13 589 water (diagonal).  
14

15  
16 590  
17

18  
19 591  
20

21 592  
22

23 593  
24

25 594  
26

27 595  
28

29 596  
30

31 597  
32

33 598  
34

35 599  
36  
37  
38  
39  
40  
41  
42  
43  
44  
45  
46  
47  
48  
49  
50  
51  
52  
53  
54  
55  
56  
57  
58  
59  
60

# Highly Sensitive Fluorescent Aptasensor for *Salmonella paratyphi A* Via DNase I-mediated Cyclic Signal Amplification

Xing Yan, Wenkai Li, Keyi Liu and Le Deng

## Graphical Abstract:

An elegant aptasensor was developed for dual fluorimetric determination of *Salmonella paratyphi A* through DNase I-assisted target recycling enlargement.

